[^{123}I]Insulin Metabolism in Normal Rats and Humans: External Detection by a Scintillation Camera

Abstract. *[^{123}I]Insulin was injected intravenously into rats and the distribution and kinetics of radioactivity were analyzed by external detection with a scintillation camera connected to a computer. When injected alone, [^{123}I]insulin was rapidly taken up by the liver and to a smaller extent by the kidneys. After reaching a maximum at 3 to 5 minutes after injection, liver radioactivity rapidly declined and free iodide appeared in the plasma. After previous saturation of the insulin receptor compartment, [^{123}I]insulin was concentrated by the kidneys only and the rate of appearance of free iodide was markedly decreased. The results demonstrate the potential usefulness of this noninvasive technique to visualize insulin interaction with the liver and kidneys and to study the rate of insulin degradation by each organ in vivo. Preliminary experiments in man demonstrate its feasibility and low radiotoxicity.*

The need for a better understanding of insulin biokinetics prompted us to investigate the feasibility of developing a noninvasive technique to follow the fate of insulin in vivo. For this purpose we labeled the hormone with ^{123}I, an isotope that emits a γ photon of adequate energy (159 KeV) for easy detection with an Anger scintillation camera. We here present an evaluation of the technique and describe the results obtained in experimental animals as well as in humans.

The ^{123}I was prepared by the ^{127}I (p,5n) $^{123}X_e \rightarrow ^{123}$I reaction (IRE, Fleurus, Belgium) and was therefore free of ^{127}I and ^{124}I and contained less than 0.2 percent ^{125}I at the time of calibration and use. Monocomponent bovine insulin (0.1 mg) was labeled with Na^{123}I (about 10 mCi in experiments with rats and 60 mCi in experiments with humans) by means of lactoperoxidase and H_2O_2 (*1*). Insulin labeled on the A14 tyrosyl residue (*2*), the only isomer known to have the same biological properties as unlabeled insulin (*3, 4*), was then rapidly purified by high-pressure liquid–reverse-phase chromatography (*5, 6*).

Carrier-free [^{123}I]insulin (about 80 μCi) (*7*) alone or mixed with a large excess (6 U) of unlabeled insulin (Actrapid) was injected in the jugular vein of anesthetized, fed young male albino rats weighing 225 to 275 g. The rats were laid prone on the high-resolution parallel collimator of a General Electric 400T Maxicamera on-line with a Simis 3 Informatek computer system. Immediately after the rats were injected, the data were recorded in a 64 by 64 matrix at a rate of two frames per minute for 30 minutes. Images were taken at selected times (Fig. 1). Regions of interest were defined over selected organs and time-activity curves were obtained and averaged for statistical variation (Fig. 2).

Within the first minutes after injection of [^{123}I]insulin alone, radioactivity was already concentrated in the liver and kidneys (Fig. 1A). Liver radioactivity reached a maximum between 3 and 5 minutes after injection, then rapidly decreased (Fig. 2A). By contrast, in rats injected with an excess of unlabeled insulin, liver radioactivity remained low and paralleled heart (that is, blood) radioactivity (Fig. 2B). Liver extraction of [^{123}I]insulin was thus a saturable process that was probably mediated by the insulin receptors (*8–10*).

After injection of [^{123}I]insulin alone, precise quantitative analysis of time-activity curves for the kidneys was hampered by superimposition of liver and right kidney activity on the one hand and of stomach and left kidney activity on the other hand (see broadening of "left kidney" image on Fig. 1B and increasing radioactivity of the "left kidney" region of interest in Fig. 2A). However, kidney activity was always lower than in rats injected with an excess of unlabeled insulin. In the latter, plasma-labeled insulin was essentially cleared by the kidneys by a nonsaturable mechanism known to proceed mainly by glomerular filtration followed by reabsorption and degradation by proximal tubular cells (*11*). In the absence of significant radioactivity uptake by the liver and stomach, "kidney" regions of interest were exclusively concerned with kidney radioactivity and both kidneys' time-activity profiles became superimposable.

As shown previously with [^{125}I]insulin, in rats injected with radioiodinated insulin alone, the rapid decrease of liver radioactivity was associated with a concomitant increase of plasma-free radioiodide concentration (*9*). It was also shown that the rate-limiting step for free iodide production was hydrolytic degradation of radioiodinated insulin itself. Indeed, free iodide appearance in the plasma was inhibited by saturation of the insulin receptor compartment with an excess of unlabeled insulin. Moreover, when rats were injected with an excess of [^{127}I]iodotyrosine in order to saturate endogenous dehalogenase activity, [^{125}I]iodotyrosine produced by degradation of the labeled insulin appeared in the plasma at the same rate as did free ^{125}I-iodide in control animals (*9*).

In the present experiments, rapid pro-

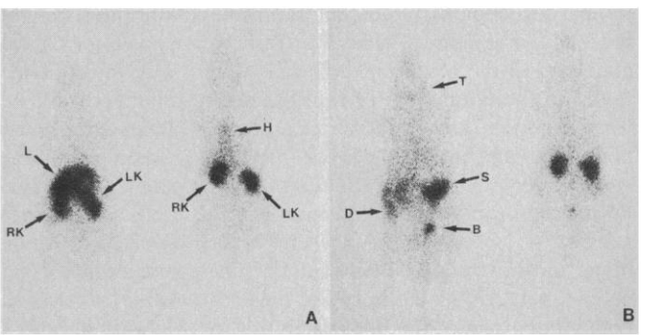

Fig. 1. Images taken (A) 3 minutes and (B) 30 minutes after intravenous injection of (rats on the left) [^{123}I]insulin alone or (rats on the right) [^{123}I]insulin mixed with an excess of unlabeled insulin; *L*, liver; *RK*, right kidney; *LK*, left kidney; *B*, bladder; *H*, heart; *S*, stomach; *D*, duodenum; *T*, thyroid.

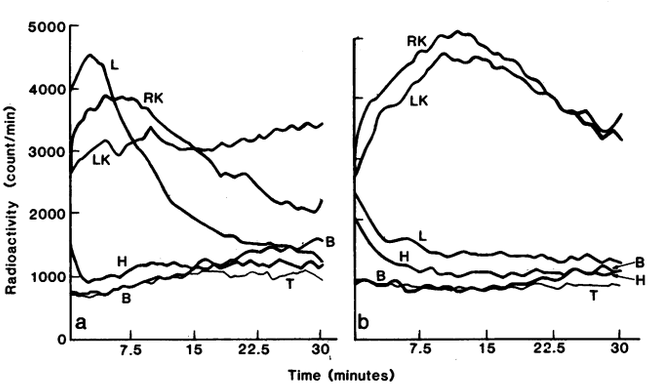

Fig. 2. The kinetics of radioactivity in the regions of interest defined in Fig. 1. (a) [^{123}I]Insulin alone and (b) [^{123}I]insulin plus excess insulin.

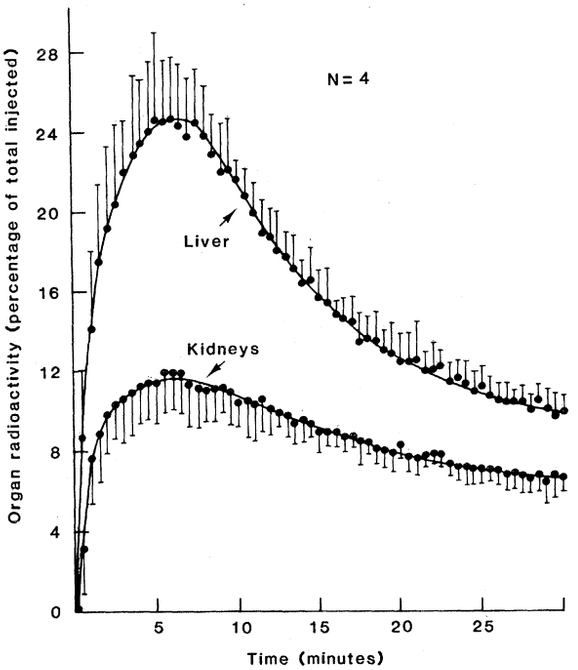

Fig. 3. Time course of estimated (see text) total radioactivity in liver and kidneys of four normal human male volunteers. These volunteers lay supine under the camera. The field of view included the heart, liver, and kidneys. All other recording parameters were similar to those in the rat studies.

duction of free ^{123}I-iodide also occurred in rats injected with [^{123}I]insulin alone, as shown indirectly by the increasing activity in selected organs such as (i) thyroid (Fig. 2A), (ii) bladder, in which accumulation of free iodide was secondary to renal excretion of iodide (Fig. 2A), and (iii) stomach. Free iodide also appeared in the proximal duodenal lumen (Fig. 1B) after iodide was taken up and secreted by the gastric mucosa (*12*).

Intravenous injection of [^{125}I]insulin followed by quantitative autoradiographic analysis demonstrated that saturable [^{125}I]insulin binding sites were most abundant in the liver, but could also be found in the epithelium of the digestive tract, adrenals, and exocrine pancreas of both fetal and adult rats. The method was not sensitive enough to detect insulin receptors in adipose and muscle tissues (*13*). Likewise, the present technique did not reveal significant [^{123}I]insulin-concentrating activity in muscle-containing parts of the body such as hip and thigh. Other receptor-rich organs probably escaped detection because of their small size or of technical limitations such as single-plane detection.

In rats injected with Na^{123}I, radioactivity was first visible in organs containing a large blood pool, and later in the gastroduodenal portion of the digestive tract, the thyroid, and the bladder. As expected, this pattern was not modified by the concomitant injection of an excess of unlabeled insulin (data not shown).

In view of the short half-life (13.3 hours) and low toxicity of the radioisotope, [^{123}I]insulin was also injected in four normal human volunteers. They were first treated with Lugol solution (30 drops per day) and, in order to minimize bladder irradiation, were requested to drink two to three liters of water the day before and the day of the experiment. [^{123}I-Tyr^{A14}]Insulin (10 mCi in 2.5 ml) that had been purified by high-pressure liquid chromatography was diluted with an equal volume of sterile saline solution containing 4 percent human serum albumin, and the mixture was sterilized by ultrafiltration through a 0.22-μm Millipore filter. A total dose of 1 to 2.8 mCi was injected in an antecubital vein at time zero. No adverse reaction was felt. Time-activity curves were obtained for regions of interest over the heart, liver, and kidneys. In all four volunteers, heart radioactivity reached a minimum between 5 to 7 minutes, corresponding to a maximum of activity in the liver and kidneys. After that maximum, the radioactivity in both liver and kidneys rapidly decreased, emphasizing that, in humans as well as rats, insulin degradation proceeds at a high rate. Phantoms of human liver and kidneys containing a known amount of ^{123}I were used to determine conversion factors between radioactivity recorded as counts per minute over a region of interest and actual radioactivity measured in microcuries in the corresponding organs. Using these factors, we calculated that maximum liver radioactivity was 24 ± 2.8 percent (mean ± standard deviation) and maximum kidney activity was 11.6 ± 1.8 percent of the total injected (Fig. 3). Corresponding figures in rats were 30 ± 4 and 15 ± 3 percent, respectively.

With regard to dosimetry, the [^{123}I]insulin is rapidly transformed into ^{123}I$^-$ (*14*). However, transient accumulation of [^{123}I]insulin in the liver and kidneys increased the dose absorbed in these organs. From the liver and kidneys acting as sources, the radioactivity absorbed by the liver was estimated at 13.5 and that by the kidneys at 40 mrad per millicurie of injected [^{123}I]insulin.

In neither rat nor man did we observe a significant accumulation of radioactivity in the gallbladder. Furthermore, radioactivity appeared earlier, and was more intense, in the stomach than in the duodenum, indicating that hepatocytes released free iodide in the blood rather than in the bile ducts.

This simple, noninvasive method thus allows study of the metabolic fate of insulin in vivo. Its potential usefulness was assessed in rats by comparing the present results with previous ones obtained with [^{125}I]insulin, killing the animals at selected times, and analyzing autoradiographs of tissues and the radiochemical composition of plasma and organ homogenates. This new technique emphasizes the prominent role of the liver and kidney in insulin disposal and the short half-life of the hormone in these organs. In view of its low radiotoxicity, this investigation procedure might be used in human diseases in order to obtain heretofore unavailable information on the uptake of insulin and its metabolic fate in liver, kidneys, and possibly other insulin target organs.

J. C. SODOYEZ
Department of Internal Medicine, University of Liege, Liege, Belgium
F. SODOYEZ-GOFFAUX
Department of Pediatrics, University of Liege
M. GUILLAUME
Cyclotron Research Center, University of Liege
G. MERCHIE
Department of Internal Medicine, University of Liege

References and Notes

1. J. I. Thorell and B. G. Johansson, *Biochim. Biophys. Acta* **251**, 363 (1971).
2. J. L. Hamlin and E. R. Arquilla, *J. Biol. Chem.* **249**, 21 (1974).
3. J. C. Sodoyez, F. Sodoyez-Goffaux, M. M. Goff, A. E. Zimmerman, E. R. Arquilla, *ibid.* **250**, 4268 (1975).
4. B. Hansen, S. Linde, O. Sonne, J. Gliemann, in *Insulin: Chemistry, Structure and Function of Insulin and Related Hormones*, D. Brandenburg and A. Wollmer, Eds. (de Gruyter, Berlin, 1980), p. 169.
5. J. Markussen and U. D. Larsen, in *ibid.*, p. 161.
6. The method of Markussen and Larsen (5) was modified to enable injection of larger volumes of the iodination mixture and to improve resolution. The iodination mixture was applied to a

MCH5 column, equilibrated with buffer A. Unreacted iodide passed through the column. After switching to buffer B, [^{123}I-Tyr^{A19}]insulin, unlabeled insulin, and [^{123}I-Tyr^{A14}]insulin were successively eluted. Elution buffers contained tris (0.5 mole/liter), phosphoric acid (0.25 mole/liter), EDTA (5 mmole/liter), and either 20 percent (buffer A) or 38 percent (buffer B) absolute ethanol; the *p*H was adjusted to 7 with tris.
7. The theoretical values of the specific activity are 41 mCi/μg for ^{123}I-labeled monoiodoinsulin and 0.37 mCi/μg for ^{125}I-labeled monoiodoinsulin.
8. S. Terris and D. F. Steiner, *J. Clin. Invest.* **57**, 885 (1976).
9. J. C. Sodoyez, F. Sodoyez-Goffaux, Y. M. Moris, *Am. J. Physiol.* **239**, E3 (1980).
10. Liver extraction of [^{123}I]insulin was inhibited by prior injection of antiserum to the insulin receptor (J. C. Sodoyez, F. Sodoyez-Goffaux, S. Treves, E. R. Kahn, in preparation).
11. M. J. Chamberlain and L. Stimmler, *J. Clin. Invest.* **46**, 911 (1967).
12. W. Meier-Ruge and F. Fridrich, *Histochemie* **19**, 147 (1969).
13. J. J. M. Bergeron, R. Rachubinski, N. Searle, D. Borts, R. Sikstrom, B. I. Posner, *J. Histochem. Cytochem.* **28**, 824 (1980); J. J. M. Bergeron *et al.*, *Endocrinology* **107**, 1069 (1980); F. Sodoyez-Goffaux, J. C. Sodoyez, C. J. De Vos, *Diabetes* **31**, 60 (1982); F. Sodoyez-Goffaux, unpublished observations.
14. I. B. Syed and F. Hosain, in *Handbook Series in Clinical Laboratory Science*, section A, *Nuclear Medicine*, D. Seligson, Ed. (CRC Press, Boca Raton, Fla., 1982), vol. 2, p. 169; J. A. Jungerman and M. C. Lagunas-Solar, *J. Radioanal. Chem.* **65**, 31 (1981).
15. This work was supported by grants from the National Fund for Scientific Research, Brussels, Belgium. We thank Ch. Fallais for the generous gift of Na^{123}I, C. R. Kahn for editorial help, and S. Segal and M. Fodor for secretarial assistance.

2 November 1982

Actin Filament Stress Fibers in Vascular Endothelial Cells in vivo

Abstract. *Fluorescence microscopy with 7-nitrobenz-2-oxa-3-diazole phallacidin was used to survey vertebrate tissues for actin filament bundles comparable to the stress fibers of cultured cells. Such bundles were found only in vascular endothelial cells. Like the stress fibers of cultured cells, these actin filament bundles were stained in a punctate pattern by fluorescent antibodies to both alpha-actinin and myosin. The stress fibers were oriented parallel to the direction of blood flow and were prominent in endothelial cells from regions exposed to high-velocity flow, such as the left ventricle, aortic valve, and aorta. Actin bundles may help the endothelial cell to withstand hemodynamic stress.*

Stress fibers (*1*), bundles of actin filaments containing myosin and α-actinin (*2*), are found in many cultured cells, but little is known about the existence of comparable actin filament bundles in living organisms. Actin bundles were recently detected in fish scales (*3*) and conifer roots (*4*) by fluorescence methods. Similar bundles have not been detected in higher vertebrates by immunofluorescence, but have been observed in the vascular endothelium by electron microscopy (*5*). The filaments in these bundles are the right size (6 to 7 nm) to be actin, and some bundles even have electron-dense bodies like stress fibers. On the other hand, the failure to detect these bundles with fluorescent antibodies to actin (*6*) casts doubt on their similarity to stress fibers. Furthermore, it has not been established whether the endothelial cell filament bundles are similar to stress fibers with respect to their distribution of myosin or α-actinin.

In this study we searched numerous vertebrate tissues for cells with actin filament bundles comparable to the stress fibers of cultured cells. We employed the fluorescence microscope with the reagent 7-nitrobenz-2-oxa-3-diazole (NBD) phallacidin as a probe (*7*). Phallacidin is an acidic derivative of phalloidine, one of the phallotoxins isolated from the mushroom *Amanita phalloides*. This toxin binds to actin filaments with high affinity (*8*). We also used fluorescent antibodies to myosin (*9*) and α-actinin (*10*) to identify the contractile proteins.

In our search we examined cryostat sections of rat cortex, cerebellum, spinal cord, sciatic nerve, epidermis, liver, bone marrow, and bovine aortic valve; smears of human peripheral blood and rat bone marrow; whole mounts of rat mesentery and brain leptomeninges; and monolayers of rat lung pleura, liver mesothelium, arachnoid mater, and bovine and chicken endothelial cells. NBD phallacidin either stained the ectoplasm of these cells more densely than the inner portion or stained the cytoplasm uniformly. Cells with the former staining pattern included motor neurons, hepatocytes, and squamous cells of the epidermis, mesothelium, pleura, and arachnoid mater. Diffuse fluorescence was found in the cell bodies of cortical and cerebellar neurons and in lymphocytes. Megakaryocytes in both smears and sections contained a lacy network not reminiscent of stress fibers.

The only actin filament bundles similar to stress fibers were found in a subset of the vascular endothelial cells of cows, chickens, dogs, rats, and a cat (Fig. 1). Although these cells vary in their morphology throughout the vasculature, each showed intense NBD phallacidin staining around its periphery (Fig. 1). In parts of the vasculature subjected to blood flow of high velocity and turbulence, the endothelial cells also contained fibers that were stained by NBD phallacidin and antibodies to actin, myosin, and α-actinin. In the cows these actin filament bundles were about 0.2 μm wide and up to 10 μm long and were always oriented parallel to the direction of blood flow. Endothelial cells with actin bundles were found in the chambers of the heart, aortic valve, and aorta (Fig. 1), but the number and size of the bundles varied, as did the shape of the cells. Actin bundles were particularly prominent in the ventricles, left atrium, and aorta. In the aorta the cells and fibers were oriented in the direction of blood flow. Endothelial cells from the vena cava were polygonal and had very few or no actin bundles (Fig. 1G).

Endothelial cell morphology varied in the different regions of the aortic valve. At the base (on either side) the cells were spindle-shaped and had very prominent actin bundles oriented parallel to the blood flow (Fig. 1, H to J). In the middle of the valve the endothelial cells were larger and oval, but the stress fibers were still oriented in the direction of flow. The cells at the valve tip were rounded and had a large nucleus and no actin fibers.

The chicken endothelial cells were similar to those of the cows in overall morphology and staining with NBD phallacidin. We stained endothelial cells of chicken aorta simultaneously with NBD phallacidin and rhodamine-labeled antibodies to chicken gizzard α-actinin (Fig. 1L) or platelet myosin (Fig. 1N). The NBD phallacidin staining of stress fibers was continuous whereas the staining with the antibodies was punctate.

The specificity of the fluorescent reagents for endothelial cells was established by showing that a 50-fold molar excess of unlabeled phalloidine competitively inhibited NBD phallacidin staining (Fig. 1O). Controls for the antibodies have been described by Herman *et al.* (*9*).

The inferior vena cava of dogs, rabbits, rats, and a cat contained almost no stress fibers. In all these species the aortic endothelial cells had actin filament bundles similar to those in the cow aorta, but the bundles were less prominent in the chambers of the heart than in cows. In most cases there were more actin filament bundles in the proximal than distal portions of the aorta, but this situation was reversed in the rat. It remains to